electronics

MDPI

Article

Clamping Force Estimation for Electro-Mechanical Brake Based on Friction Torque Fusion Approach

Giseo Park [1], Sooyoung Kim [2,*] and Jungwoo Kim [1]

[1] School of Mechanical Engineering, University of Ulsan, Ulsan 44610, Republic of Korea; eloq123@ulsan.ac.kr (G.P.); kjw6410@mail.ulsan.ac.kr (J.K.)
[2] Department of Mechanical Systems Engineering, Sookmyung Women's University, Seoul 04310, Republic of Korea
* Correspondence: syk@sookmyung.ac.kr

Abstract: Electromechanical brakes (EMB) are anticipated to become the standard brake system in the future, gaining favor among researchers and automobile manufacturers due to their numerous advantages. However, to achieve cost competitiveness, expensive load cells used to measure the clamping force on the disc must be replaced with a clamping force estimation algorithm. To do this, an algorithm is first developed to estimate the pad contact point, which represents the point of contact between the pad and the disc, to determine where the clamping force occurs. Subsequently, this paper proposes a novel Kalman filter approach utilizing friction torque fusion for clamping force estimation. Specifically, the estimation performance is enhanced by incorporating both dynamic and static friction torque models. The proposed estimation algorithm is validated by comparing its results with the actual clamping force measured using a load cell sensor. Furthermore, experimental tests are conducted to confirm whether the proposed estimation algorithm maintains its performance under various control reference conditions, and overall, the estimation error was within about 5% in this paper.

Keywords: electromechanical brake; clamping force estimation; Kalman filter; friction torque

check for updates

Academic Editor: Davide Astolfi

Received: 5 November 2024
Revised: 9 January 2025
Accepted: 14 January 2025
Published: 17 January 2025

Citation: Park, G.; Kim, S.; Kim, J. Clamping Force Estimation for Electro-Mechanical Brake Based on Friction Torque Fusion Approach. *Electronics* **2025**, *14*, 348. https://doi.org/10.3390/electronics14020348

Copyright: © 2025 by the authors. Licensee MDPI, Basel, Switzerland. This article is an open access article distributed under the terms and conditions of the Creative Commons Attribution (CC BY) license (https://creativecommons.org/licenses/by/4.0/).

1. Introduction

The electro-mechanical brake (EMB), a type of brake-by-wire system, is currently being extensively studied by many automobile-related industries for its potential use in future vehicles [1]. At present, most EMB control systems employ a closed-loop control with a cascaded structure [2]. These systems typically comprise a motor current controller, a motor angular velocity controller and a clamping force controller, arranged in that order, and are generally feedback-based. As the control response speed tends to decrease the further out it is in the system hierarchy, the cascaded structure is used to address this limitation [3].

If the clamping force information can be obtained indirectly without relying on a load cell sensor, the price competitiveness of the EMB system is expected to improve significantly [4,5]. Moreover, beyond the cost-related issues, clamping force sensors face challenges such as a reduced accuracy at high temperatures and difficulties in structural integration [6]. Therefore, to enhance the cost competitiveness of the EMB system and ensure its stability, a reliable method for indirectly estimating the clamping force is highly needed.

1.1. Literature Review

Various methods for estimating the clamping force of EMB systems have been introduced in numerous papers since the late 1990s. One of the earliest and most notable

methods, introduced in [7], involves the use of a clamping force characteristic curve based on the motor rotation angle. Later, Ref. [8] proposed a method to adapt this characteristic curve to the brake pad temperature by utilizing a temperature sensor embedded within the brake pad. Additionally, Ref. [5] incorporated the hysteresis phenomenon into the characteristic curve, further refining the estimation process.

However, these characteristic curve-based methods have a significant limitation: the coefficients of the characteristic curve need to be adjusted depending on various environmental factors, such as the motor's internal temperature or the brake pad's thickness.

To address these limitations, Ref. [9] introduced a method combining the clamping force characteristic curve with the Kalman filter. Subsequently, clamping force estimation methods employing switching extended state observers [10,11] and unknown input disturbance observers [12,13] were developed. Furthermore, the adaptive Kalman filter method proposed in [14] was applied to EMB clamping force estimation to better adapt to environmental changes.

For these observer-based estimation methods, which rely on the state equations of the EMB system, accurately describing the internal behavior of the EMB is crucial. However, the friction torque of the EMB exhibits entirely different characteristics in static and dynamic states, making accurate modeling a challenging task.

1.2. Contributions

The research objectives of this paper are primarily divided into two main goals. First, an algorithm is developed to estimate the contact point between the pad and the disc, enabling the accurate determination of when the clamping force occurs. The clamping force can also be modeled as a characteristic curve function of the motor rotation angle. In this case, the pad contact point is a crucial factor that significantly impacts the overall accuracy of the characteristic curve.

The second primary research objective is the development of a linear Kalman filter algorithm for real-time clamping force estimation. This paper introduces a novel method for smoothly and precisely combining different friction torque models in both dynamic and static states using weight factors. Through this approach, the aim is to achieve accurate clamping force estimates in both steady and transient states.

1.3. Contents of Paper

The overall structure of this paper is as follows. Section 2 introduces the EMB dynamics modeling process used. Sections 3 and 4 cover the pad contact point estimation and the Kalman filter for clamping force estimation, respectively. Section 5 analyzes the experimental results on the test bench and Section 6 presents the conclusion of this paper.

2. EMB Dynamics Modeling

2.1. EMB Torque Dynamics

The motor type of the EMB used in this paper is a surface permanent magnet synchronous motor (SPMSM) and the overall structure of the EMB is shown in Figure 1. Also, some specifications of the SPMSM used are summarized in Table 1. The motor torque T_m of the EMB is equal to the sum of the load torque $k_{cl}F_{cl}$, the friction torque T_f, and the inertial torque $J\dot{\omega}_m$ of the EMB system. In particular, the load torque occurs when the brake pad is in contact with the disc and a clamping force is applied, and it can be expressed as the clamping force multiplied by a load-torque constant k_{cl}. During braking, heat is generated due to the friction between the brake pads and discs. This heat causes thermal expansion and changes in material properties, which can affect the value of the load-torque constant

k_{cl} [8]. Therefore, creating a look-up table of k_{cl} according to braking conditions is one of the future tasks.

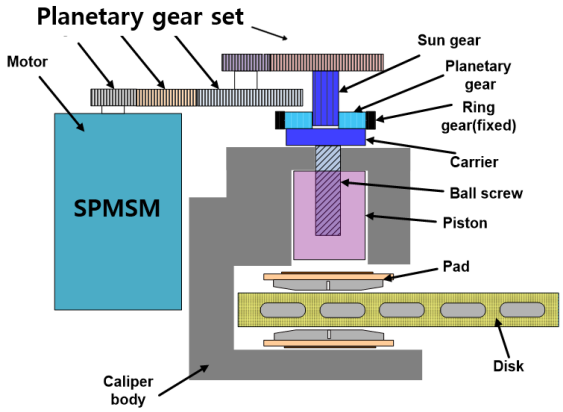


Figure 1. Overall structure of EMB.

Table 1. Motor specifications.

Quantity	Value
Maximum motor voltage	10.4 V
Maximum motor current	50 A
Maximum motor power	285 W
Maximum motor torque	1.6 Nm

In the case of EMB, the information about the clamping force between friction pads and brake discs is essential for accurate brake system control [4]. However, although a load cell sensor for clamping force exists, the additional cost is considerable, so its price competitiveness is significantly lower than that of existing hydraulic brake systems. The torque balance equation for the EMB system is as follows [15]:

$$T_m = J\dot{\omega}_m + T_f + k_{cl}F_{cl} \tag{1}$$

Here, J is the moment of inertia and ω_m is the motor angular velocity. The torque generated as a resistance to the rotational movement of the motor and gear parts within the EMB system can be considered the friction torque. There are various models of friction torque depending on the characteristics of the system, and the friction torque model considered most suitable for the EMB system is as follows.

$$T_f = \begin{cases} \left(T_{f0} + GF_{cl}\right) sign(\omega_m) + B\omega_m \; if \; |\omega_m| \geq \varepsilon \\ T_E \qquad\qquad\qquad\qquad otherwise \end{cases} \tag{2}$$

where T_{f0}, G, and B are the load-independent coulomb friction torque, friction-load dependency and viscous damping coefficient, respectively. Equation (2) intuitively simplifies the EMB friction torque formula proposed in [16], which considers both the load dependency and the relationship between friction and speed.

Dynamic friction torque refers to a motion situation where the motor rotation angle moves even a little and static friction torque refers to a situation where the motor is almost stationary. They are distinguished by the magnitude of the real-time motor angular velocity $|\omega_m|$. When the rotating body is stopped (the magnitude of motor angular velocity $|\omega_m|$ is smaller than a very small constant ε), a friction torque equal to the external torque T_E occurs. At this time, the external torque means the difference between the motor torque and the load torque: $T_E = T_m - k_{cl}F_{cl}$.

2.2. Determination of EMB Parameters

In the case where the EMB system parameters, the moment of inertia J and the damping coefficient B, need to be determined in a situation where the load cell is not installed, the following process is proposed. First, since the clamping force is zero in the clamping situation before the brake pad contacts the disc, the friction torque is modeled as follows: $T_f = T_{f0} + B\omega_m$. Accordingly, the EMB torque balance equation in the clamping situation before the pad contacts the disc is as follows.

$$T_m - T_{f0} = J\dot{\omega}_m + B\omega_m \tag{3}$$

At this time, T_{f0} can be specified as the corresponding value of motor torque T_m when the angular velocity ω_m just starts to occur. In order to determine the moment of inertia J and the damping coefficient B in the torque balance equation at the same time, the least squares method can be applied as follows.

$$\begin{bmatrix} J & B \end{bmatrix}^T = P = \left(W^T W\right)^{-1} W^T Y \tag{4}$$

where $W = \begin{bmatrix} \dot{\omega}_m & \omega_m \end{bmatrix}$ and $Y = T_m - T_{f0}$.

The parameter values J and B can be output from the parameter vector P. In order to extract data from the no-load section (when the clamping force is zero) only, only the section where the clamping force command just starts to occur is used as the data extraction section, as shown in Figure 2a. Based on the EMB sensor signals obtained from the no-load section between 19.54 s and 19.56 s of Figure 2a, the determined values of J and B are 1.22×10^{-5} kg·m^2 and 1.61×10^{-4} Nm·s/rad, respectively.

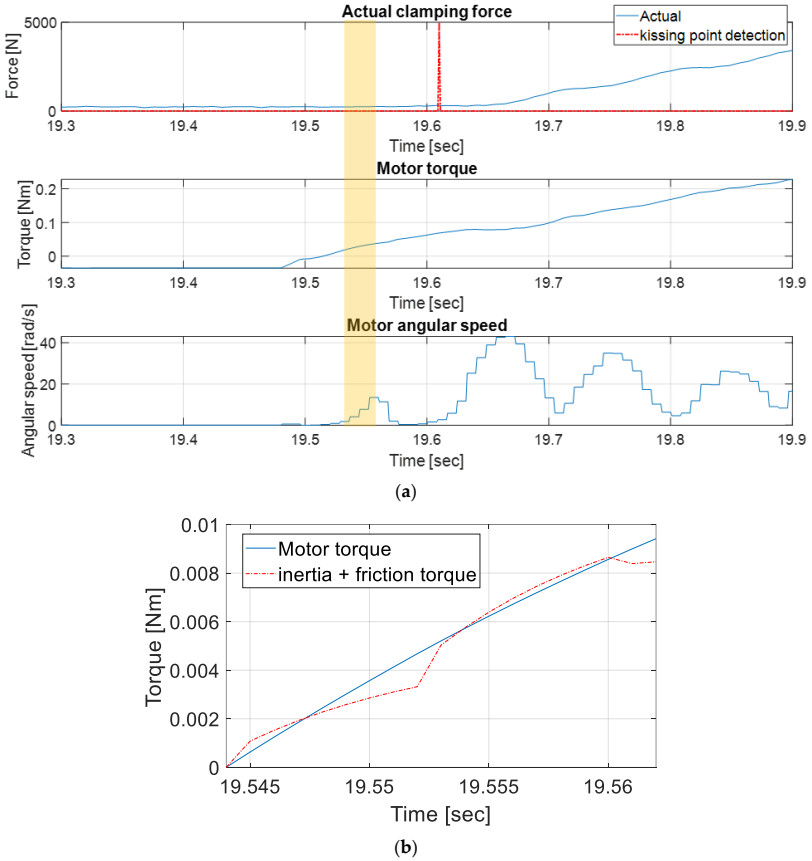


Figure 2. Data extraction area for EMB parameter determination: (**a**) EMB sensor signals, and (**b**) comparison of torque signals (motor torque $T_m - T_{f0}$ and inertia + friction torque $J\dot{\omega}_m + B\omega_m$).

Through Equation (3), it can be confirmed that J and B are accurate values if the torque value $J\dot{\omega}_m + B\omega_m$ including the determined J and B matches the torque signal $T_m - T_{f0}$. Figure 2b shows that the torque signals $T_m - T_{f0}$ and $J\dot{\omega}_m + B\omega_m$ match within the data extraction area between 19.54 s and 19.56 s, which confirms that the determined J and B are accurate values that can be used to estimate the clamping force.

3. Pad Contact Point Estimation

As introduced earlier, the pad contact point provides various types of information on the design of the control system of electric brakes. In the existing clamping force estimation studies [1–5], the clamping force was generally expressed as a polynomial function of third or higher order for the motor rotation angle.

At this time, because the pad contact point represents the starting point of the clamping force characteristic curve, it is a very important factor in determining the accuracy of the overall clamping force estimate value.

In addition, the accurate information on the timing of pad contact is also required for braking control techniques that slightly reduce the motor torque value to prevent strong shock when there is contact between the pad and the disc.

The contact point estimation technique, based on the awareness of the braking direction, and the strategy identifying the pad contact point, based on the differential current signal, were introduced in [9,17], respectively. In this paper, we propose the following three conditions to determine the motor rotation angle at which the pad comes into contact with the disc and clamping force begins to be generated more precisely than when using the existing methods.

(1) Motor torque satisfies the range $T_{m,low} \leq T_m$

(2) Motor torque change rate satisfies the range $\frac{dT_m}{dt} \leq \left.\frac{dT_m}{dt}\right|_{upp}$

(3) Direction in which the pad presses the disc (clamping situation)

When all three conditions above are satisfied, the pad contact point can be detected. The motor rotation angle at the point of contact with this pad is set to $\theta_{m,pc}$.

If the clamping force command speed increases rapidly, early kissing point detection may occur. To prevent this, a look-up table is used in which the magnitude of thresholds $T_{m,low}$ and $\left.\frac{dT_m}{dt}\right|_{upp}$ increase linearly as the clamping force command speed increases. In addition, since the no-load section where the pad contact point detection occurs is the initial section where the motor torque value is very small, the characteristics of these thresholds do not change depending on the specific EMB hardware. Therefore, the thresholds $T_{m,low}$ and $\left.\frac{dT_m}{dt}\right|_{upp}$ that only change with respect to the clamping force command speed are used.

Figure 3 shows the actual clamping force, motor torque and motor torque change rate during a typical braking command situation. For general braking commands excluding rapid clamping force commands, a phenomenon occurs in which the motor torque change rate drops rapidly in the moment the pad touches the disc. However, when a sudden clamping force command is given, this drop in the motor torque change rate does not appear clearly, making it unsuitable for use in estimating the pad contact point.

At about 34 s and 42 s in Figure 3b, the motor torque T_m in that section is sufficiently larger than the threshold value $T_{m,low}$. At the same time, the motor torque rate $\frac{dT_m}{dt}$ in Figure 3c represents a value sufficiently smaller than the threshold $\left.\frac{dT_m}{dt}\right|_{upp}$. Accordingly, at the 34 s and 42 s sections, all three conditions necessary for estimating the pad contact point described above are satisfied, and the pad contact point estimation is activated immediately.

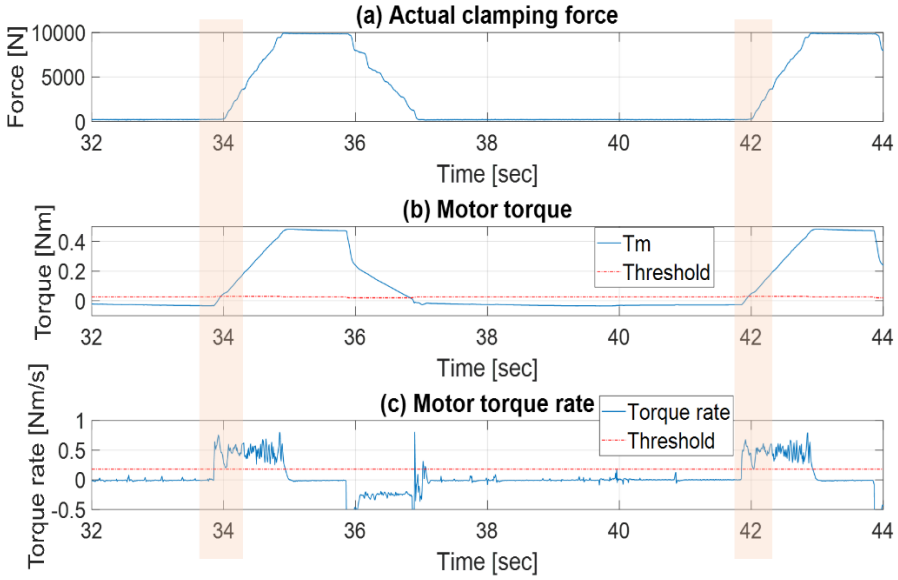


Figure 3. Typical braking command situation: (**a**) actual clamping force, (**b**) motor torque, and (**c**) motor torque rate.

Figure 4 shows the difference between the estimation method in the existing papers [1–3] and our proposed method. Since the existing method activates the estimation whenever the change in motor torque exceeds a certain level, frequent enable signals are generated.

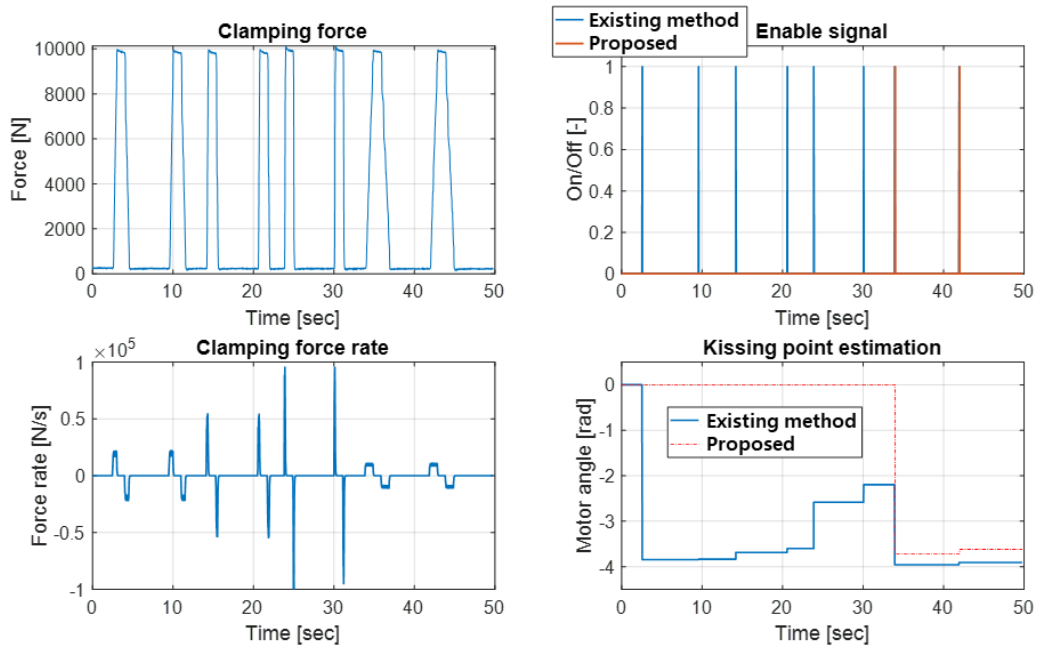


Figure 4. Comparison of existing and proposed methods for pad contact point estimation.

Accordingly, the estimated pad contact point $\theta_{m,pc}$ fluctuates significantly. In contrast, the proposed method generates an enable signal only when all three specific conditions introduced above are satisfied, so the fluctuation of the estimated $\theta_{m,pc}$ is not severe. In this paper, this estimated real-time pad contact point $\theta_{m,pc}$ is directly used to accurately determine the point at which the clamping force estimation occurs.

4. Kalman Filter Design

In this paper, we propose the Kalman filter algorithm as an algorithm for real-time clamping force estimation. The Kalman filter has a similar form to the Luenberger observer, but its main feature is that it calculates the Kalman gain in real time based on statistical methods to minimize estimation errors. To implement the Kalman filter, the motor rotation angle, motor angular velocity and motor torque signal information are used.

The Kalman filter, using the torque balance Equation (1) of the EMB system, is designed in this paper. In addition to the clamping force to be estimated, the motor angular velocity is included in the state variable vector of the Kalman filter: $x_k = \begin{bmatrix} F_{cl,k} & \omega_{m,k} \end{bmatrix}^T$. Also, the measured value of the Kalman filter corresponds to the motor angular velocity ω_m.

4.1. Structure of Kalman Filter

A linear Kalman filter in the discrete time system is given as shown below.

$$x_k = F_{k-1}x_{k-1} + G_{k-1}x_{k-1} + w_{k-1} \tag{5}$$

$$y_k = H_k x_k + v_k \tag{6}$$

Figure 5 summarizes the entire process of the discrete Kalman filter algorithm. The prediction step is a step to predict the estimated value using only system model information, and the correction step is a step to correct the estimated value through the measured value y_k.

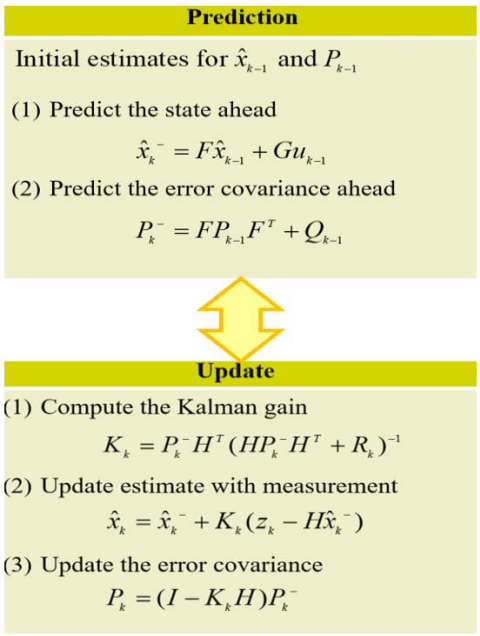


Figure 5. Kalman filter process.

Equations (5) and (6) are expressed as EMB torque balance models (7) and (8) in this paper, respectively.

$$\begin{bmatrix} F_{cl,k+1} \\ \omega_{m,k+1} \end{bmatrix} = \begin{bmatrix} 1 & 0 \\ -T_s\frac{k_{cl}}{J} & 1 \end{bmatrix} \begin{bmatrix} F_{cl,k} \\ \omega_{m,k} \end{bmatrix} + \begin{bmatrix} 0 \\ T_s\frac{T_{m,k}-T_{f,k}}{J} \end{bmatrix} \tag{7}$$

$$\omega_m = \begin{bmatrix} 0 & 1 \end{bmatrix} \begin{bmatrix} F_{cl,k} \\ \omega_{m,k} \end{bmatrix} \tag{8}$$

where T_s is the sampling time of the discrete system. The estimated clamping force $\hat{F}_{cl}$ is output in real time by the proposed Kalman filter. Through this, the final clamping force estimate value $\hat{F}_{cl}$ is designed to have a value greater than 0 only in the motor rotation angle larger than the estimated pad contact point $\theta_{m,pc}$.

4.2. Friction Torque Fusion Approach

As the friction torque in (2) has different formulas in dynamic and static states, discontinuities that are different from the actual state may appear when the state changes.

Therefore, this paper seeks to utilize a new weight factor to represent continuous friction torque values similar to reality when changing between dynamic and static states. The weight factor α of the friction torque is designed as follows.

$$\alpha = \text{sat}\left[\frac{|\omega_m| - \varepsilon + \tau}{2\tau}\right] \tag{9}$$

In Figure 6, the form of the saturation function of the weight factor α in (9) is schematized, and according to this, the weight factor has a value between 0 (meaning a completely static state) and 1 (meaning a complete dynamic state). First, the parameter ε is the angular velocity threshold that determines the stationary and moving states. It is set to a small velocity threshold value by utilizing the Karnopp remedy for zero velocity detection [16]. In this paper, ε is determined to be 10 rad/s.

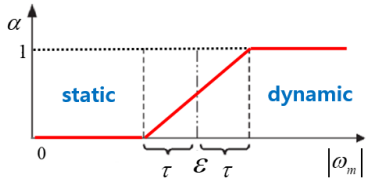


Figure 6. Weighting factor of friction torque.

Also, the parameter τ is a value to prevent abrupt transitions between the stationary and moving states of the clamping force estimation value. The larger the parameter τ, the slower the transition from the stationary to the moving state of the clamping force estimation value becomes. Therefore, in the section where the actual clamping force value begins to occur, it is necessary to evaluate whether the transition point from the stationary to the moving state of the estimated clamping force value matches the actual clamping force.

In (9), there may be a problem that the situation in which the motor rotation angle θ_m changes slowly while having a small $|\omega_m|$ is incorrectly detected as a static state (in reality, since the motor rotation angle changes slowly, it has to be determined as a dynamic state).

To solve this problem, the accumulated change amount of the motor rotation angle has to be observed in real time even in the static state. First, at every moment when the static state ($\alpha = 0$) begins to be determined, the motor rotation angle at that point is set to the initial position θ_{m_ini}. Then, when θ_m differs by a certain amount from the initial position θ_{m_ini}, the weighting factor is changed to a dynamic state ($\alpha = 1$).

The final friction torque T_f, which has a weighted sum form, is defined as follows and is directly used in (7).

$$T_f = \alpha\Big(\Big(T_{f0} + GF_{cl}\Big)sign(\omega_m) + B\omega_m\Big) + (1-\alpha)T_E \tag{10}$$

Compared with the existing methods, such as the general Kalman filter technique [2] and the characteristic curve technique [5], the proposed estimation method can show a tendency closer to the actual clamping force at the transition points between the stationary

and moving states. This is because the fusion of static and dynamic friction torque models proposed in this paper contributes to accurately describing the behavior of the actual EMB.

5. Experiments

The EMB test bench, which consists of EMB units, discs, and controller area network (CAN)-based data transmission and reception equipment, is used in this paper for EMB clamping force estimation experiments. The EMB experimental environment is configured as shown in Figure 7. The main parameters of the EMB used in experiments are summarized in Table 2.

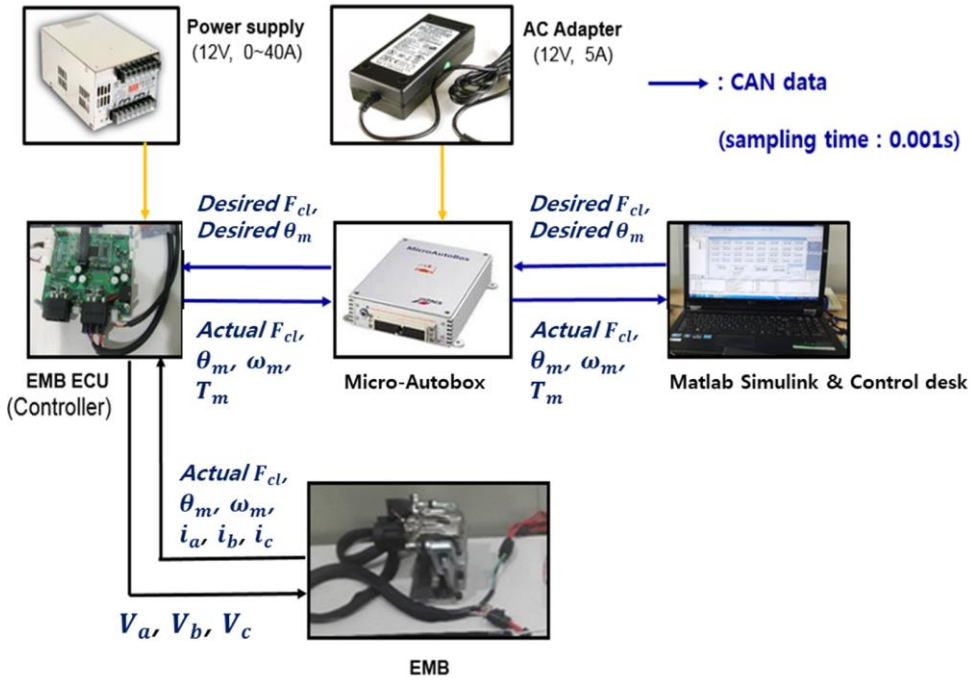


Figure 7. Schematic diagram of the EMB experimental environment.

Table 2. EMB Parameters for clamping force estimation.

Parameter	Quantity	Value
J	Moment of inertia	1.22×10^{-5} kg·m^2
B	Viscous damping coefficient	1.61×10^{-4} Nm·s/rad
G	Friction load dependency	2.9369×10^{-6} m
T_{f0}	Load-independent coulomb friction torque	0.0093 Nm
k_{cl}	Load-torque constant	3.9159×10^{-5} m

To verify the accuracy of the clamping force estimation for various clamping force command profiles, experimental tests 1 and 2 are performed in this paper. The clamping force estimation result of the proposed algorithm is compared with the actual value measured from the load cell sensor.

Experimental test 1 represents step-up and step-down scenarios between 0 N and 22,000 N at an instantaneous speed of 4000 N/s. The clamping force repeats a step shape with a hold time of 1 s, and the overall clamping situation (at 10~30 s and 55~75 s) and release situation (at 30~55 s and 75~100 s) occur continuously. Through experimental test 1, the clamping force estimation accuracy in the steady state and transient state can be confirmed clearly.

Figure 8 shows the actual and estimated clamping force signals together over the entire time. The root mean square (RMS) error over the entire section is recorded as 5.17%. Also,

as shown in Figure 9, we can specifically check how well the estimated value matches the actual value, depending on the actual clamping force area. Figure 9a,b show the satisfactory high estimation accuracy in clamping and releasing situations, respectively.

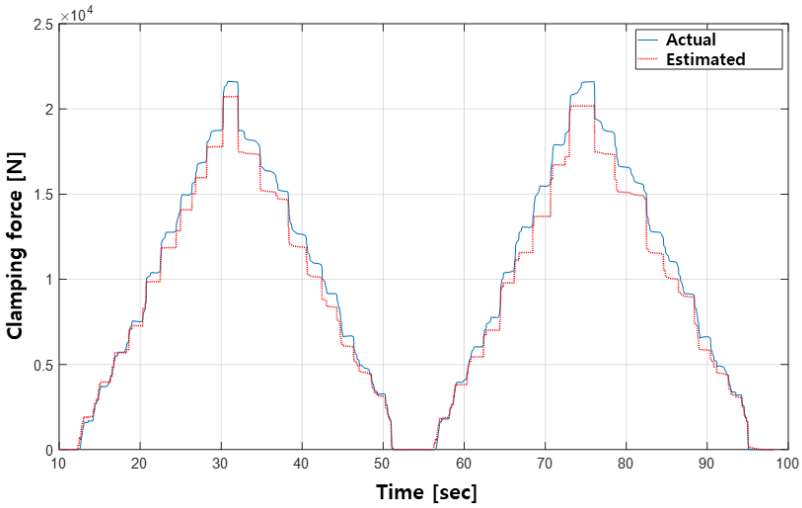


Figure 8. Clamping force estimation result in experimental test 1.

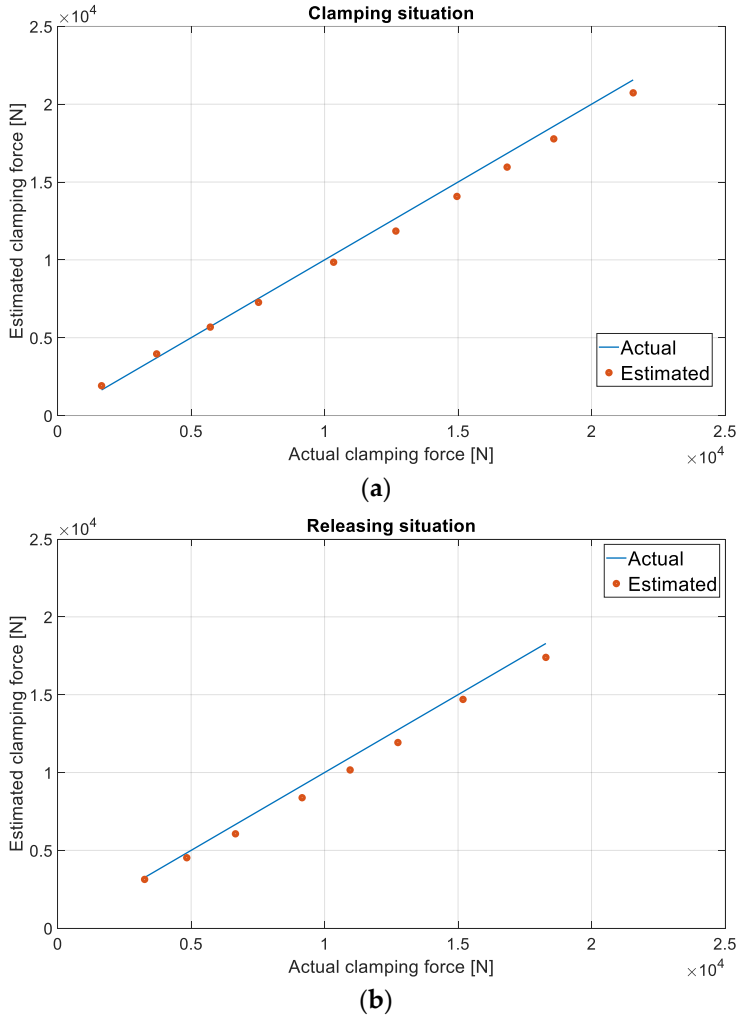


Figure 9. Estimated clamping force versus actual clamping force in experimental test 1: (**a**) clamping situation and (**b**) releasing situation.

In Figure 10, in order to check the accuracy of the pad contact point estimation algorithm, the sections around 5.1 s and 48.1 s when the clamping force begins to occur are zoomed in. It can be seen that the pad contact point estimation is activated at the moment the clamping force occurs and $\theta_{m,pc}$ is instantly designated as the motor rotation angle value at the corresponding contact point.

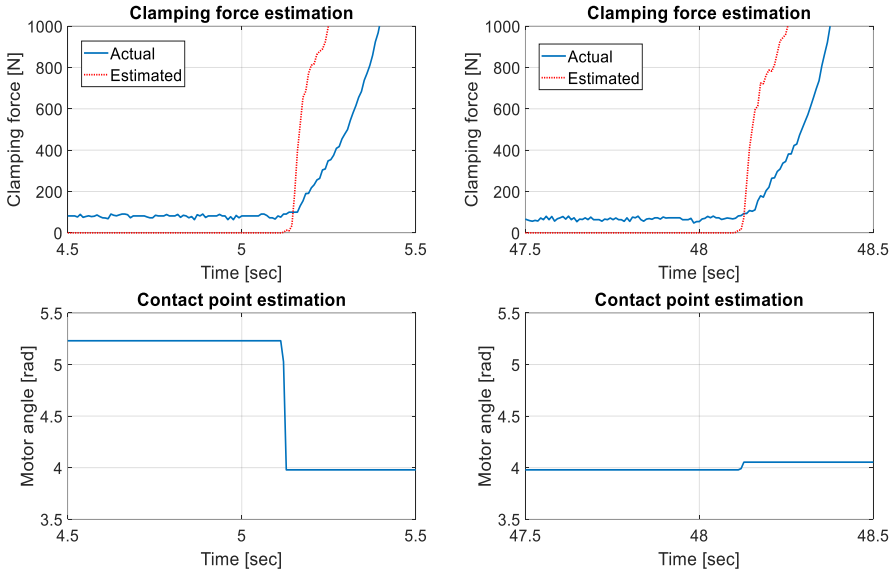


Figure 10. Pad contact point estimation in experimental test 1.

Experimental test 2 is a test in which the actual clamping force has a ramp wave shape between 10,000 N and 22,000 N and, like the previous experimental test 1, the estimation performance in both the steady and transient states can be confirmed.

In the transient state, the clamping force is changing at a speed of 36,000 N/s, and in the steady state (sections maintained at 10,000 N and 22,000 N), each has a hold time of 1 s.

First, Figure 11 shows the actual and real-time estimated clamping force during the entire time of experimental test 2. In this test, the overall RMS error of the clamping force estimation corresponds to 5.15%. Additionally, the estimation accuracy of the pad contact point in experimental test 2 is shown in Figure 12. It can be seen that when the actual clamping force begins to occur at around 5.5 s and 13.1 s, respectively, the pad contact point estimation is immediately activated and the motor rotation angle at that point is immediately selected as the value of $\theta_{m,pc}$.

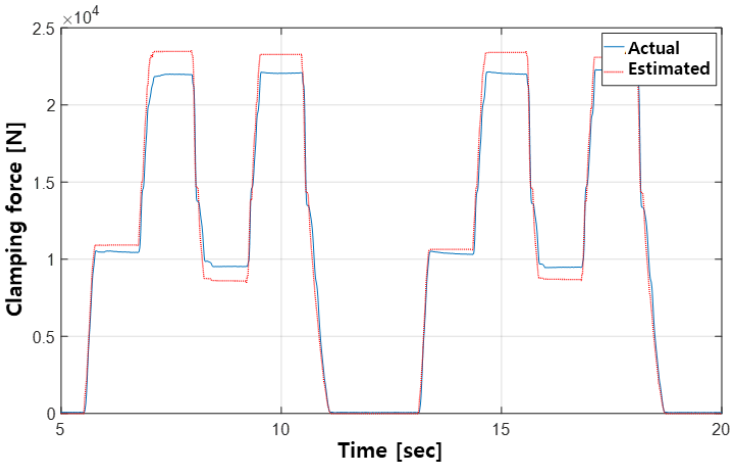


Figure 11. Clamping force estimation result in experimental test 2.

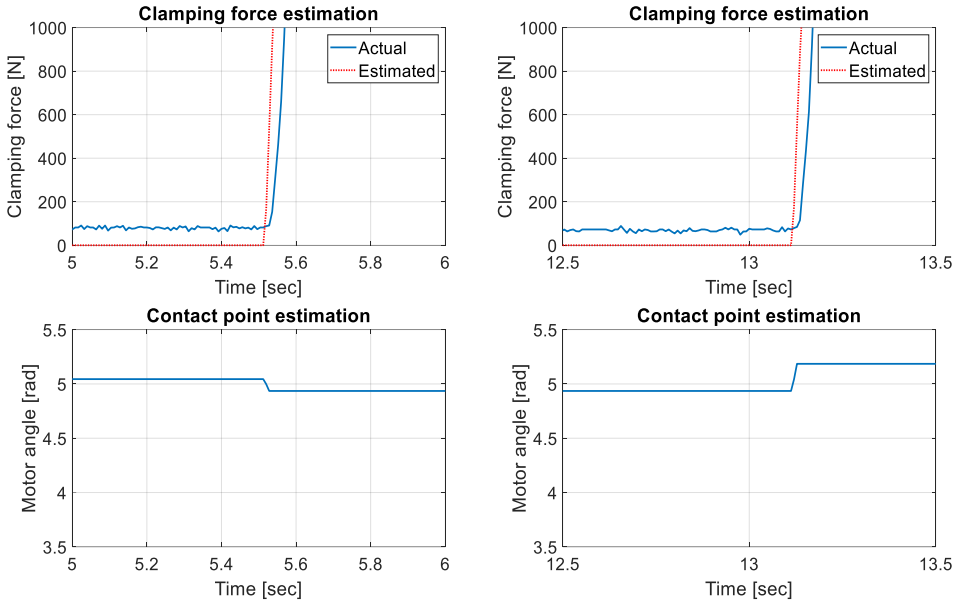


Figure 12. Pad contact point estimation in experimental test 2.

6. Conclusions

In this paper, a new estimation algorithm is developed to accurately identify the contact point between the brake pad and the disc. Additionally, based on EMB dynamics modeling, a linear Kalman filter algorithm that ensures continuous and smooth friction torque transitions between dynamic and static states is newly proposed.

The pad contact point estimation method presented in this paper actively leverages the physical phenomena of motor torque and its rate of change at a specific moment to precisely detect when the EMB clamping force begins to act.

Furthermore, the Kalman filter for clamping force estimation employs a weighted sum of friction torques in both dynamic and static states. The main advantages of the proposed estimation algorithm are as follows:

(1) By meticulously modeling the friction torque in the static state, a high performance in clamping force estimation during steady-state operation can be achieved.
(2) When transitioning between dynamic and static states, abrupt changes in the estimated clamping force value can be avoided.

The effectiveness of the proposed estimation algorithm is verified through test bench experiments, which include various clamping force commands. To further enhance the accuracy of the clamping force estimation provided by the proposed Kalman filter algorithm, an accurate calibration process for various friction torque parameters will be necessary. In addition, in order to achieve the optimality of the fusion of the two friction torque models proposed in this paper, we plan to apply the interacting multiple model (IMM) Kalman filter algorithm in a new way in the future.

In conclusion, the proposed pad contact point detection and real-time clamping force estimation algorithms are expected to significantly contribute to the mass production of EMB systems in the future.

Author Contributions: Conceptualization, G.P.; data curation, G.P.; formal analysis, G.P.; funding acquisition, G.P.; investigation, S.K.; methodology, G.P.; project administration, G.P.; resources, S.K.; software, G.P.; supervision, G.P.; validation, G.P.; visualization, J.K.; writing—original draft, S.K.; writing—review and editing, G.P. All authors have read and agreed to the published version of the manuscript.

Funding: This research was partly supported by a "Regional Innovation Strategy (RIS)" grant through the National Research Foundation of Korea (NRF), funded by the Ministry of Education (MOE), (2021RIS-003) and the Korea Institute of Energy Technology Evaluation and Planning (KETEP) grant, funded by the Korea government (MOTIE), (20224000000440, sector coupling energy industry advancement manpower training program).

Data Availability Statement: Data are contained within the article.

Conflicts of Interest: The authors declare no conflicts of interest.

References

1. Park, G.; Choi, S.; Hyun, D. Clamping Force Estimation Based on Hysteresis Modeling for Electro-Mechanical Brakes. *Int. J. Automot. Technol.* **2017**, *18*, 883–890. [CrossRef]
2. Saric, S.; Bab-Hadiashar, A.; Hoseinnezhad, R. Clamp-Force Estimation for a Brake-by-Wire System: A Sensor-Fusion Approach. *IEEE Trans. Veh. Technol.* **2008**, *57*, 778–786. [CrossRef]
3. Jo, C.; Hwang, S.; Kim, H. Clamping-Force Control for Electromechanical Brake. *IEEE Trans. Veh. Technol.* **2010**, *59*, 3205–3212. [CrossRef]
4. Park, G.; Hyun, D.; Choi, S. Development of Clamping Force Estimation Algorithm and Clamp-force Sensor Calibration on Electromechanical Brake Systems. *Trans. KSAE* **2016**, *24*, 365–371. [CrossRef]
5. Ki, Y.; Lee, K.; Cheon, J.; Ahn, H. Design and Implementation of a new Clamping force estimator in Electro-Mechanical Brake systems. *Int. J. Automot. Technol.* **2013**, *14*, 739–745. [CrossRef]
6. Hoseinnezhad, R.; Bab-Hadiashar, A.; Rocco, T. Real-Time Clamp Force Measurement in Electromechanical Brake Calipers. *IEEE Trans. Veh. Technol.* **2008**, *57*, 770–777. [CrossRef]
7. Schwarz, R.; Isermann, R.; Bohm, J.; Nell, J.; Rieth, P. Modeling and Control of an Electromechanical Disk Brake. *SAE Tech. Paper* **1998**, *980600*, 14. [CrossRef]
8. Saric, S.; Bab-Hadiashar, A.; Walt, J. Estimating clamp force for brake-by-wire systems: Thermal considerations. *Mechatronics* **2009**, *19*, 886–895. [CrossRef]
9. Kwon, S.; Lee, S.; Lee, J.; Kum, D. Accurate State Estimation for Electro-Mechanical Brake Systems. *J. Elect. Eng. Technol.* **2019**, *14*, 889–896. [CrossRef]
10. Xu, Z.; Gerada, C. Enhanced Force Estimation for Electromechanical Brake Actuators in Transportation Vehicles. *IEEE Trans. Power Electron.* **2021**, *36*, 14329–14339. [CrossRef]
11. Xu, Z.; Gerada, C. Enhanced Estimation of Clamping-Force for Automotive EMB Actuators Using a Switching Extended State Observer. *IEEE Trans. Ind. Electron.* **2024**, *71*, 2220–2230. [CrossRef]
12. Li, Y.; Shim, T.; Shin, D.; Lee, S.; Jin, S. Control System Design for Electromechanical Brake System Using Novel Clamping Force Model and Estimator. *IEEE Trans. Veh. Technol.* **2021**, *70*, 8653–8668. [CrossRef]
13. Wei, W.; He, T.; Pal, A. Real-time Clamping Force Estimation of Brake- by-Wire System for Electric Autonomous Vehicles. In Proceedings of the 2023 American Control Conference (ACC), San Diego, CA, USA, 31 May–2 June 2023; pp. 1018–1023.
14. Liu, K.; Liu, Z.; Tan, X.; Liu, S.; Wu, G. A fusion estimation method of clamping force for electro-mechanical brake system based on adaptive Kalman filtering. *Trans. Inst. Meas. Cont.* **2024**, 01423312241291096. [CrossRef]
15. Baek, S. Comparative Evaluation of Electro-Mechanical Brake Clamping Force Estimation and Sensor Compensation Control Method for High-Speed-Train. *IEEE Access* **2024**, *12*, 45644–45653. [CrossRef]
16. Line, C.; Manzie, C.; Good, M. Electromechanical Brake Modeling and Control: From PI to MPC. *IEEE Transac. Control Syst. Technol.* **2008**, *16*, 446–457. [CrossRef]
17. Zhang, Y.; Chen, Z.; Wu, J.; Zhang, Y. *Gap Adjustment Strategy for Electromechanical Brake System Based on Critical Point Identification*; SAE Technical Paper 2024-01-2320; SAE International: Warrendale, PA, USA, 2024. [CrossRef]

Disclaimer/Publisher's Note: The statements, opinions and data contained in all publications are solely those of the individual author(s) and contributor(s) and not of MDPI and/or the editor(s). MDPI and/or the editor(s) disclaim responsibility for any injury to people or property resulting from any ideas, methods, instructions or products referred to in the content.